ACIN

Repetitive nonlinear control for linear scanning micro mirrors

Richard Schroedter[a], Markus Schwarzenberg[a], Jan Grahmann[a], Thilo Sandner[a], and Klaus Janschek[b]

[a]Fraunhofer Institute for Photonic Microsystems (FhG-IPMS), AMS, Microscanner R&D, Dresden, Germany
[b]Institute of Automation, Faculty of Electrical and Computer Engineering, Technische Universität Dresden, 01062 Dresden, Germany

ABSTRACT

Various scanning applications like LIDAR sensors, OCT systems and laser projectors require a repeated periodic linear scanning trajectory performed by a quasi-static micro mirror. Since most MOEMS systems have inherent nonlinearities like a progressive spring stiffness and the quadratic voltage-deflection-relation of electrostatic drives, a nonlinear control scheme as presented in our previous paper [1] significantly reduces parasitic oscillations of the resonance frequency and enables a high resolution raster scan combining a quasi-static axis with a cardanic mounted resonant axis. In this paper we address a novel control scheme using a flatness-based feedback control enhanced by a plug-in repetitive controller for the linear scanning axis. We demonstrate the applicability of this feedback control for a quasi-static moving micro mirror with electrostatic staggered vertical comb drives using a microcontroller-based driver. On-chip piezoresistive sensors serve as position feedback [2]. We compare different scan trajectories and repetition rates with respect to the linearity and repeatability showing the robustness of the proposed control regime. Furthermore we discuss the advantage of this method to reduce the individual chip characterization for ramping up mass production.

Keywords: repetitive, nonlinear closed-loop control, quasi-static, electrostatic, micro mirror, staggered vertical comb drive, piezoresistive sensor

1. INTRODUCTION

Micro scanning mirrors are in focus for many applications like light deflection and ranging (LIDAR) [3,4], optical coherence tomography (OCT) [5] and laser projectors [6]. Quasi-static microscanners hold the advantage of static positioning and dynamic trajectory tracking in comparison to state of the art resonant Lissajous scanners [7]. But due to their extreme low damping, feedback control is required for enabling high precision tracking. Actual research offers numerous control approaches such as linear controllers [8,9] and nonlinear methods like exact linearization and flatness-based controllers [10–12] or sliding mode and robust controllers [13,14]. Those control schemes operate immediately on the actual error. But most applications with scanning mirrors demand periodic repeated trajectories, that are beneficial for iterative learning and repetitive control regimes. These algorithms diminish deviations using the tracking error of past periods iteratively in comparison to instantaneous controllers mentioned before. Repetitive control has been applied for hard disk drives [15] and scanning probe microscopes [16], but rarely for scanning micro mirrors.

Therefore, we demonstrate a novel control repetitive nonlinear control scheme for quasi-static scanning micro mirrors. In previous works we concentrated on open-loop and closed-loop control strategies using flatness-based control [1, 12, 17, 18]. In this paper, we combine the nonlinear control with a plug-in repetitive controller. The performance is verified for different trajectories on the quasi-static axis of a microscanner using on-chip piezoresistive sensor feedback for closed-loop control. The paper is organized as follows: In section 2 we introduce the microscanner describing its functionality and identifying the parameter used for real-time control. We present the repetitive nonlinear control algorithm in section 3. The experimental results are shown in 4. In section 5 we discuss the benefit for mass production. Finally, the contribution is summarized in section 6.

Further author information: (Send correspondence to Richard Schroedter)
Richard Schroedter: E-mail: richard.schroedter@ipms.fraunhofer.de, Telephone: + 49 351 8823 196
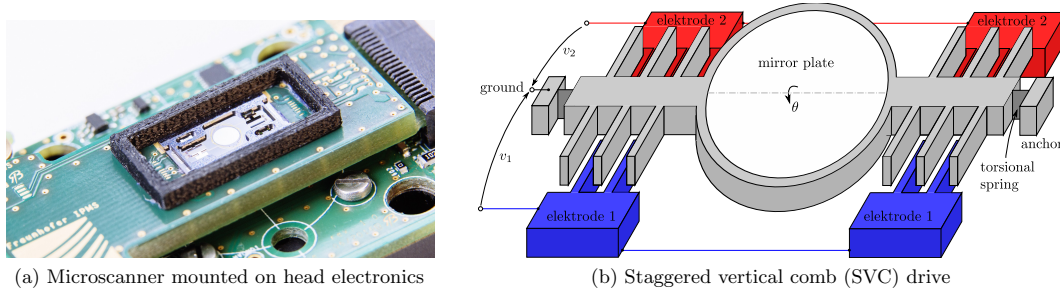Klaus Janschek: E-mail: klaus.janschek@tu-dresden.de, Telephone: +49 351 463 34025

For further information contact: schroedter@acin.tuwien.ac.at, https://orcid.org/0000-0003-3259-4571

(a) Microscanner mounted on head electronics

(b) Staggered vertical comb (SVC) drive

Figure 1: Quasi-static scanning micro mirror and driving principle

2. QUASI-STATIC SCANNING MICRO MIRROR

The examined quasi-static scanning micro mirror is shown in Fig. 1a. The micro-electro-mechanical-system (MEMS) device is fabricated in a fully CMOS compatible process from single crystalline silicon. The mirror can tilt up to $\theta = \pm 8°$ actuated by electrostatic comb drives, whose outer electrodes are shifted down about once the substrate height of 75 μm, as it is shown in Fig. 1b. This is realized by bonding a second wafer on the device wafer resulting in a staggered vertical comb (SVC) drive, as described by JUNG et al. in [19]. A cardanic mounted inner axis operates in a resonant mode [7]. This enables a 2D raster scan, as presented in [12]. Near the torsional springs piezoresistive sensors, as introduced in [2], serve as position feedback for the closed-loop control.

The quasi-static axis of the microscanner is modeled with the following nonlinear differential equation (cf. [18]):

$$J\ddot{\theta} + b\dot{\theta} + \tau_{\mathrm{s}}(\theta) = \frac{1}{2}C_1'(\theta)\,v_1^2 + \frac{1}{2}C_2'(\theta)\,v_2^2, \qquad \tau_{\mathrm{s}}(\theta) = \int_0^\theta k(\theta')\,\mathrm{d}\theta'. \tag{1}$$

In Eq. (1) J denotes the mirrors torque inertia, b describes the viscous damping coefficient of the surrounding air, $\tau_{\mathrm{s}}(\theta)$ defines the spring torque by integrating the spring stiffness $k(\theta)$. The nonlinear stiffness, given in Fig. 2a, is modeled with ANSYS®. The stiffness $k(0) = J\omega_0 = 3.66\,\mu\mathrm{Nm/rad}$ at zero deflection is derived from a decay measurement of an impulse stimulation, as well as the damping $b = 1.96 \times 10^{-11}\,\mathrm{Nms}$. The mirror eigenfrequency is $f_0 = 188.9\,\mathrm{Hz}$ and the quality factor is $Q = 157$. $C_1'(\theta)$ and $C_2'(\theta)$ are the capacitance derivatives of both SVC electrodes (Fig. 2b), determined from the static deflection characteristic with the relation $C_{1,2}'(\theta) = 2\tau_{\mathrm{s}}(\theta)/v_{1,2}^2$.

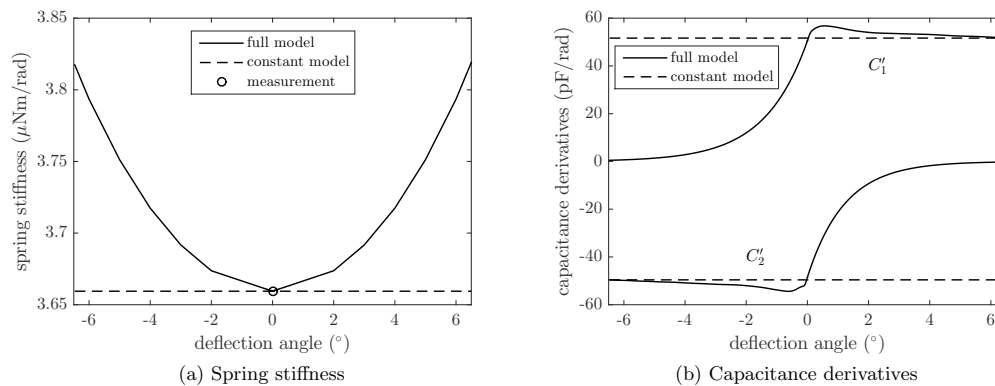(a) Spring stiffness

(b) Capacitance derivatives

Figure 2: Parameter curves of nonlinear and constant mirror model

3. REPETITIVE NONLINEAR CONTROL ALGORITHM

The proposed repetitive nonlinear control algorithm is based on the flatness-based feed forward control with output stabilization, as it is published in [12]. The full control structure is shown in Fig. 4.

a) Nonlinear control The trajectory generator provides a periodic triangle or saw tooth trajectory with jerk limitation using the third order polynomial $\theta_\mathrm{d}(t) = a_0 + a_1 t + a_2 t^2 + a_3 t^3$ in the time span $[0; T]$, as introduced in [17]. The flatness-based *feed forward control* creates the desired acceleration u_d as follows:

$$u_\mathrm{d} = \ddot{\theta}_\mathrm{d} + w_\mathrm{d}, \qquad w_\mathrm{d} = \frac{b}{J}\dot{\theta}_\mathrm{d} + \frac{\tau_\mathrm{s}(\theta_\mathrm{d})}{J}. \tag{2}$$

To reduce the position error $e = \theta_\mathrm{d} - \hat{\theta}$ and the velocity error $\dot{e} = \dot{\theta}_\mathrm{d} - \dot{\hat{\theta}}$, we use the following PD-controller and its poles are placed as according to the eigenfrequency $\omega_0 = 2\pi f_0$ with $k_\lambda > 0$:

$$\Lambda(e, \dot{e}) = P\,e + D\,\dot{e}, \qquad P = 3\lambda^3, \qquad D = 3\lambda, \qquad \lambda = k_\lambda \cdot \omega_0. \tag{3}$$

The resulting correction of the controller $\Lambda(e, \dot{e})$ is added to the desired acceleration, obtaining:

$$u = u_\mathrm{d} + \Lambda(e, \dot{e}). \tag{4}$$

According to the acceleration u the drive voltage is switched (*comb switch*) to one of the electrodes as follows:

$$v_1 = \begin{cases} \sqrt{\dfrac{2\,J\,u}{C_1'(\theta_\mathrm{d})}} & \text{for} \quad u > 0 \\ 0 & \text{for} \quad u \le 0 \end{cases}, \qquad v_2 = \begin{cases} 0 & \text{for} \quad u > 0 \\ \sqrt{\dfrac{2\,J\,u}{C_2'(\theta_\mathrm{d})}} & \text{for} \quad u \le 0 \end{cases}. \tag{5}$$

The actual mirror state is observed with a *reduced observer* using the acceleration $\ddot{\theta}_\mathrm{d} + \Lambda(e, \dot{e})$ and the measured deflection angle $\tilde{\theta}$ as input. The observer is implemented as follows:

$$\dot{\hat{\theta}} = \int \left(\ddot{\theta}_\mathrm{d} + \Lambda(e, \dot{e}) + l_2\left(\hat{\theta} - \tilde{\theta}\right) \right) \mathrm{d}\,t, \qquad \hat{\theta} = \int \left(\dot{\hat{\theta}} + l_1\left(\hat{\theta} - \tilde{\theta}\right) \right) \mathrm{d}\,t. \tag{6}$$

The poles of the observer gain $\boldsymbol{l} = (l_1, l_2)^\mathrm{T}$ are placed with the ACKERMANN formula at a positive multiple of the mirror eigenfrequency using $k_{\hat{\lambda}} > 1$:

$$l_1 = 2\hat{\lambda}, \qquad l_2 = \hat{\lambda}^2, \qquad \hat{\lambda} = k_{\hat{\lambda}} \cdot \omega_0. \tag{7}$$

For open-loop control P and D are set to zero.

b) Repetitive control The repetitive controller (RC) is plugged in the proportional "P" error channel e of the controller $\Lambda(e, \dot{e})$. Consequently the new controller becomes:

$$\Lambda'(e + e_\mathrm{RC}, \dot{e}) = P \cdot (e + e_\mathrm{RC}) + D\,\dot{e}. \tag{8}$$

The examined "plug-in" type of the RC, shown in Fig. 3, was proposed by TOMIZUKA et al. in [15] and further designed by TSAI et al. in [20]. Accordingly, the repetitive controller is given as follows:

$$C_\mathrm{RC}(s) = K_\mathrm{L}(s) \cdot \frac{K_\mathrm{Q}(s) \cdot e^{-Ts}}{1 - K_\mathrm{Q}(s) \cdot e^{-Ts}}. \tag{9}$$

With proving the stability of the closed-loop, the RC is designed in the frequency domain using the LAPLACE variable s. We suppose, that the system is exactly linearized and comes sufficiently close to the desired trajectory by applying jerk limited trajectories and the flatness-based feed forward control. Therefore, we assume the exactly linearized system $G_0(s)$ performing like a double integrator $1/s^2$.
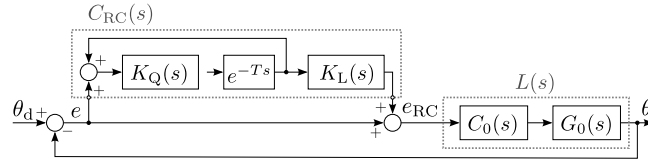
Figure 3: Repetitive controller in the linear closed-loop

Together with the PD-controller $C_0(s)$ we get the following linear system equations:

$$G_0 = \frac{1}{s^2}, \quad C_0(s) = P + D\frac{s}{1 + T_N s}, \quad L(s) = C_0(s) \cdot G_0(s), \quad S_0(s) = \frac{1}{1 + L(s)}, \quad T_0(s) = \frac{L(s)}{1 + L(s)}. \quad (10)$$

The RC itself is an error generator for the existing feedback control, adding a filtered error of the last periods to the actual error. The time shift e^{-Ts} is realized with a data storage. Since the continuous error generation can destabilize the control loop, the following *stabilizing filter* $K_Q(s)$ of second order is implemented:

$$K_Q(s) = K_{Q,0}(s) \cdot e^{+\tau_Q s} \quad \text{with} \quad K_{Q,0}(s) = \frac{V_Q}{1 + 2d_Q\frac{s}{\omega_Q} + \frac{s^2}{\omega_Q^2}}. \quad (11)$$

The stabilizing filter $K_{Q,0}(s)$ is designed by evaluating the *regeneration spectrum* $R(\omega) < 1$, as introduced by SRINIVASAN et al. in [21] and described by TSAI et al. in [20]:

$$R(\omega) = |K_{Q,0}(j\omega) \cdot S_0(j\omega)| < 1. \quad (12)$$

By choosing the damping $d_Q = \sqrt{2}/2$ the maximum frequency is given by:

$$\omega_Q = \frac{\omega_S}{\sqrt[4]{(V_Q \cdot S_{0,\text{max}})^2 - 1}}. \quad (13)$$

In Eq. (13) ω_S denotes the intersection frequency of the sensitivity function with zero decibel: $S_0(\omega_S) = 0\,\text{dB}$. $S_{0,\text{max}}$ is the global maximum $S_{0,\text{max}} = \max(|S_0(\omega)|)$ of the sensitivity function (cf. [20]). The stabilizing filter leads to a time delay, which is compensated using the positive time shift τ_Q, designed as follows:

$$\tau_Q = \frac{\pi}{2\omega_Q}. \quad (14)$$

Furthermore, the repetitive control dynamic is adjusted with the *learning gain* $K_L(s)$:

$$K_L(s) = V_L \cdot e^{+\tau_L s}. \quad (15)$$

The positive time shift τ_L compensates the time delay induced by the closed-loop control $T_0(j\omega) = |T_0(j\omega)| \cdot e^{j\varphi_T}$. We design τ_L within the working area $[0; \omega_Q]$ of the repetitive controller using the following relation:

$$\tau_L = \frac{-\varphi_T(\omega_Q)}{\omega_Q}. \quad (16)$$

The maximum learning gain V_L in the working area $[0; \omega_Q]$ is calculated as follows:

$$V_L = \frac{2\cos[\varphi_T(\omega_Q) + \omega_Q\tau_L]}{\max(|T_0(\omega_Q)|)}. \quad (17)$$

Since the positive time shifts of τ_Q and τ_L cannot be realized, the structure, presented in Fig. 3, is transformed to an equivalent having only negative time shifts, as shown in Fig. 4. The condition $T > \tau_Q + \tau_L$ must be fulfilled.

For the presented micro scanner with the eigenfrequency 188.9 Hz we derived the optimal control parameter given in Tab. 1. We found $S_{0,\text{max}} = 1.15$ and $\varphi_T(\omega_Q) = 77°$. This design of the repetitive controller is stable, because the maximum $R_{\text{max}} = 0.87$ of the regeneration spectrum $R(\omega)$ is below 1 resp. 0 dB.

For further information contact: schroedter@acin.tuwien.ac.at, https://orcid.org/0000-0003-3259-4571

ACIN

PD controller		repetitive controller					
k_λ	$k_{\hat{\lambda}}$	V_Q	d_Q	ω_Q	τ_Q	V_L	τ_L
0.22	7	1	0.71	$1272\,\mathrm{s}^{-1}$	$1.24\,\mathrm{ms}$	2.88	$1.06\,\mathrm{ms}$

Table 1: Control parameter (bold parameters are tuned for optimal result)

4. EXPERIMENTAL RESULTS

The experimental results proof the impact of the proposed repetitive nonlinear control scheme in reducing tracking errors. The experimental setup is shown in Fig. 4. The control is performed with the microcontroller-based driver electronics at 12 kHz control frequency, as presented in [1]. The on-chip integrated piezoresistive sensor is used for position feedback. The control performance is verified with an optical reference measurement setup using a *position sensitive device* (PSD) with a standard deviation lower than 1 millidegree, as it was figured out in [12].
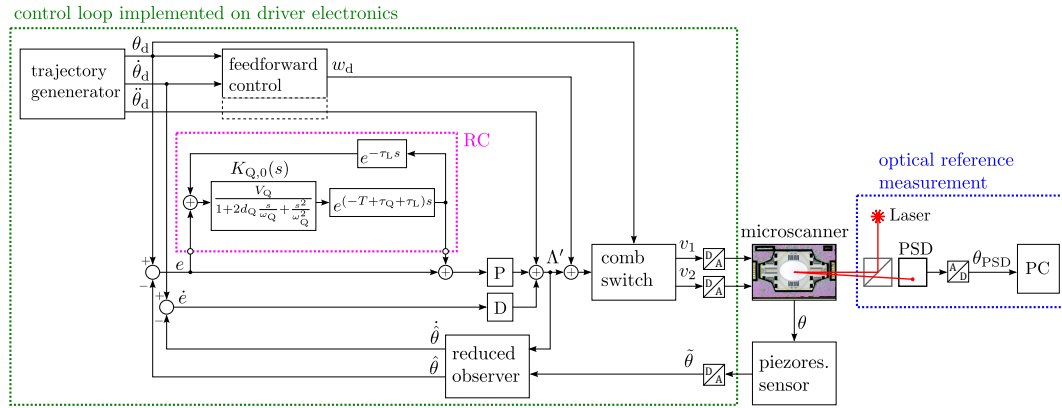

Figure 4: Experimental setup with implemented control loop and optical reference measurement

Fig. 5 demonstrates the experimental results of the error $\theta_d - \theta_{PSD}$ for a 10 Hz triangle and saw tooth trajectory comparing open-loop (OL), closed-loop (CL) and closed-loop with repetitive controller (CL with RC) operation. Tab. 2 summarizes the results of the peak-to-peak errors in the linear trajectory part (linearity error) and the repeatability error of 100 periods for different repetition rates. All errors are given in ‰ with relation the corresponding total linear deflection of $2\,\theta_{lin}$.

	triangle trajectory			saw tooth trajectory		
repetition rate	10 Hz	20 Hz	30 Hz	10 Hz	20 Hz	30 Hz
linear time	90 %	80 %	70 %	90 %	80 %	70 %
$\theta_{max}\,\vert\,\theta_{lin}$	6°|5.6°	6°|5.1°	6°|4.7°	6°|5.9°	6°|5.8°	6°|5.6°
peak-to-peak linearity error of 100 periods						
open-loop (OL)	10.9 ‰	11.0 ‰	10.1 ‰	8.4 ‰	6.5 ‰	4.9 ‰
closed-loop (CL)	4.3 ‰	5.0 ‰	5.5 ‰	1.5 ‰	2.8 ‰	3.8 ‰
closed-loop with repetitive controller (CL with RC)	3.5 ‰	4.1 ‰	4.8 ‰	1.0 ‰	1.5 ‰	2.8 ‰
peak-to-peak repeatability error of 100 periods						
open-loop (OL)	0.6 ‰	0.6 ‰	0.8 ‰	1.0 ‰	0.6 ‰	0.7 ‰
closed-loop (CL)	1.0 ‰	1.0 ‰	1.1 ‰	0.9 ‰	1.0 ‰	1.0 ‰
closed-loop with repetitive controller (CL with RC)	1.5 ‰	1.2 ‰	1.3 ‰	1.3 ‰	1.2 ‰	1.2 ‰

Table 2: Experimental linearity and repeatability errors of 100 periods with [10, 20, 30] Hz repetition rate
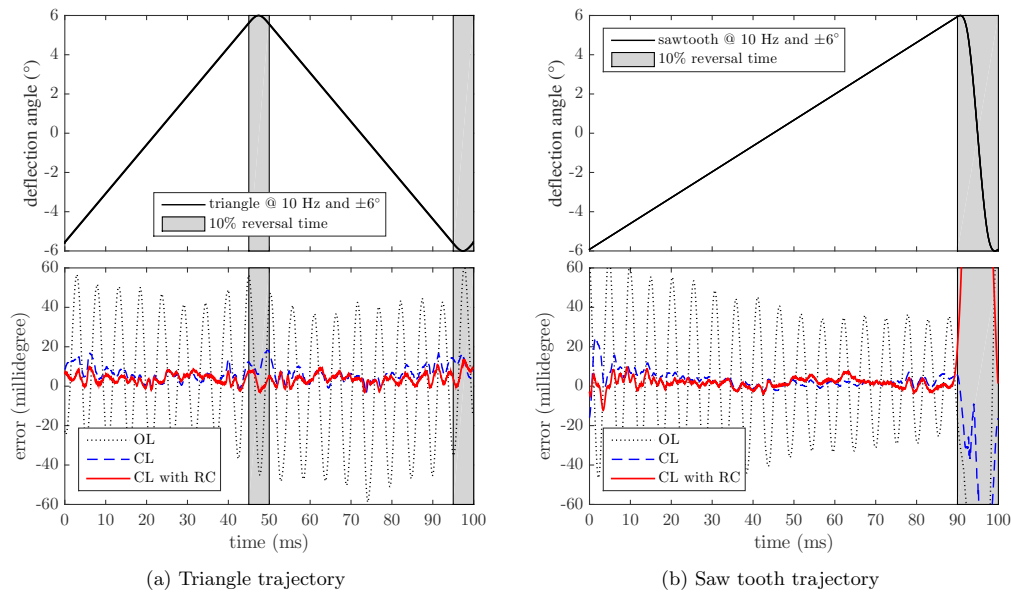
(a) Triangle trajectory

(b) Saw tooth trajectory

Figure 5: Experimental results for 10 Hz triangle and saw tooth trajectories with 90 % linear time (upper graphs) and deviation from reference (lower graphs) using open-loop (OL), closed-loop (CL) and closed-loop with repetitive controller (CL with RC)

The major reduction of residual oscillations at the mirror eigenfrequency f_0 is achieved by closing the loop. By activating the repetitive controller the linearity error is further reduced about 1/3. At the same time the repeatability error slightly increases. Nevertheless, the gain in performance remains $6\ldots 30\,\%$ according to the trajectory considering both errors, linearity and repeatability.

5. DISCUSSION

A major advantage of the RC is the ability to compensate deviations due to the static model nonlinearities like the progressive stiffness and the nonlinear comb capacitances. Since the model inversion of the flatness-based control method requires a complete model at all operation points to enable high precise tracking control, a time consuming individual chip characterization is conducted. In further experiments we have set the spring stiffness and capacitances derivatives to constant values, as shown in Fig. 2 (constant model). These results of the repetitive nonlinear control (CL with RC) are demonstrated in Fig. 6 using the desired trajectories shown in Fig. 5 (upper graphs). We identify a remarkable error reduction of factor 6.8 with a final linearity error of 3.7‰ for the triangle trajectory and a reduction of factor 13.3 with a final linearity error of 1.3‰ for the saw tooth trajectory.

The experimental results proof the positive "learning" effect of the RC. The RC is able to decrease nontransient deviations of the model in particularly, because it is placed in the proportional "P" channel of the nonlinear controller. As a conclusion the proposed repetitive nonlinear control scheme enables avoiding an individual chip characterization. Nevertheless, a high precise model of the piezoresistive sensor is required. Configuring the sensor as a WHEATSTONE full bridge sensor, it manifests a major linear characteristic, as GRAHMANN et al. present in [2]. Finally, the linearity error of 1‰ for 10 Hz saw tooth operation enables 1000 pixels for the quasi-static axis. Combining the quasi-static axis with an inner cardanic mounted resonant axis, this microscanner concept has great potential for high resolution imaging and sensor applications.

(a) Triangle trajectory during linear time

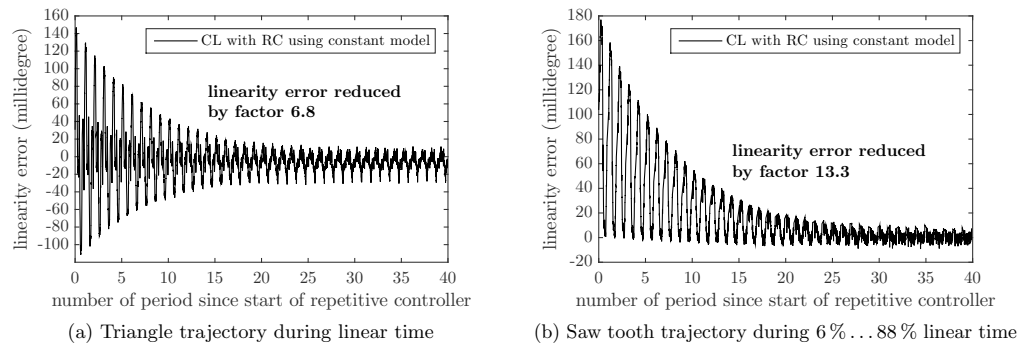(b) Saw tooth trajectory during 6 % . . . 88 % linear time

Figure 6: Experimental linearity error evolution of closed-loop with repetitive controller (CL with RC) using constant mirror model for the 10 Hz trajectories (cf. Fig. 5 upper graphs). Errors during reversal time are not shown.

6. SUMMARY

In this paper we presented a promising repetitive control method for linear scanning quasi-static micro mirrors with inherent nonlinearities in the system model. We demonstrated the stable design of the plug-in repetitive controller for a flatness-based feedback control regime with a reduced observer using the approximation of an exactly linearized system model. The experimental results show a prominent positive effect on the linearity error offset, which is caused by model uncertainties. Consequently, the individual chip characterization may be simplified, assuming an adequate knowledge of the piezoresistive position feedback characteristics. Further steps are considering a temperature compensation and increasing the control frequency for high speed scanning.

REFERENCES

[1] Schroedter, R., Schwarzenberg, M., Dreyhaupt, A., Barth, R., Sandner, T., and Janschek, K. ", Microcontroller based closed-loop control of a 2D quasi-static/resonant microscanner with on-chip piezo-resistive sensor feedback," in [*Proc. SPIE*], **10116**, 1011605–1011605–11 (2017).

[2] Grahmann, J., Dreyhaupt, A., Drabe, C., Schroedter, R., Kamenz, J., and Sandner, T. ", MEMS-mirror based trajectory resolution and precision enabled by two different piezoresistive sensor technologies," in [*MOEMS and Miniaturized Systems XV*], *Proc. SPIE* **9760**, 976006–976006–11 (2016).

[3] Weiss, U. and Biber, P. ", Plant detection and mapping for agricultural robots using a 3D {LIDAR} sensor," *Robotics and Autonomous Systems, Special Issue ECMR* **59**(5), 265–273 (2011). Special Issue {ECMR} 2009.

[4] Hofmann, U. and Aikio, M. ", Biaxial tripod mems mirror and omnidirectional lens for a low cost wide angle laser range sensor,", 323–332, Springer Berlin Heidelberg (2012).

[5] Sun, J., Guo, S., Wu, L., Liu, L., Choe, S.-W., Sorg, B. S., and Xie, H. ", 3D in vivo optical coherence tomography based on a low-voltage, large-scan-range 2D MEMS mirror," *Opt. Express OSA* **18**(12), 12065–12075 (2010).

[6] Davis, W. O., Sprague, R., and Miller, J. ", MEMS-based pico projector display," in [*IEEE/LEOS International Conference on Optical MEMs and Nanophotonics*], 31–32 (2008).

[7] Schenk, H., Sandner, T., Drabe, C., Klose, T., and Conrad, H. ", Single crystal silicon micro mirrors," *physica status solidi* **6**(3), 728–735 (2009).

[8] Milanović, V., Kasturi, A., Yang, J., and Hu, F. ", Closed-loop control of gimbal-less mems mirrors for increased bandwidth in lidar applications," *Proc. SPIE* **10191**, 10191 – 10191 – 13 (2017).

[9] Pannu, S., Chang, C., Muller, R. S., and Pisano, A. P. ", Closed-loop feedback-control system for improved tracking in magnetically actuated micromirrors," in [*IEEE/LEOS International Conference on Optical MEMS*], 107–108 (2000).

For further information contact: schroedter@acin.tuwien.ac.at, https://orcid.org/0000-0003-3259-4571

ACIN

[10] Agudelo, C. G., Zhu, G., Packirisamy, M., and Saydy, L.", Flatness-based control of an electrostatic torsional micro-mirror with voltage feedback," in [*50th Midwest Symposium on Circuits and Systems*], 654–657 (2007).

[11] Ma, Y., Islam, S., and Pan, Y.-J.", Electrostatic torsional micromirror with enhanced tilting angle using active control methods," *IEEE ASME Transactions on Mechatronics* **16**(6), 994–1001 (2011).

[12] Schroedter, R., Roth, M., Janschek, K., and Sandner, T.", Flatness-based open-loop and closed-loop control for electrostatic quasi-static microscanners using jerk-limited trajectory design," *Mechatronics: Special Issue on MEMS Dynamics and Control* (2017).

[13] Sane, H. S., Yazdi, N., and Mastrangelo, C. H.", Robust control of electrostatic torsional micromirrors using adaptive sliding-mode control," in [*Proc. SPIE*], **5719**, 115–126 (2005).

[14] Chen., H., Sun, W. J., Sun, Z. D., and Yeow, J. T. W.", Second-order sliding mode control of a 2D torsional MEMS micromirror with sidewall electrodes," *Journal of Micromech. Microeng. 23 015006* , 9–19 (2013).

[15] Tomizuka, M., Tsao, T.-C., and Chew, K.-K.", Analysis and synthesis of discrete-time repetitive controllers," *Journal of Dynamic Systems, Measurement, and Control* **111**(3), 353–358 (1989).

[16] Aridogan, U., Shan, Y., and Leang, K. K.", Design and analysis of discrete-time repetitive control for scanning probe microscopes," *Journal of Dynamic Systems, Measurement, and Control* **131**, 061103 (2009).

[17] Schroedter, R., Janschek, K., and Sandner, T.", Jerk and Current Limited Flatness-based Open Loop Control of Foveation Scanning Electrostatic Micromirrors," in [*International Federation of Automation and Control (IFAC) Conference*], 2685–2690 (2014).

[18] Schroedter, R., Sandner, T., Janschek, K., Roth, M., and Hruschka, C.", Real-time closed-loop control for micro mirrors with quasistatic comb drives," in [*MOEMS and Miniaturized Systems XV*], *Proc. SPIE* **9760**, 976009–976009–13 (2016).

[19] Jung, D., Kallweit, D., Sandner, T., Conrad, H., Schenk, H., and Lakner, H.", Fabrication of 3d comb drive microscanners by mechanically induced permanent displacement," in [*MOEMS and Miniaturized Systems VIII*], David L. Dickensheets, Harald Schenk, W. P., ed., *Proc. SPIE* **7208**, 72080A–72080A–11 (2009).

[20] Tsai, M.-C. and Yao, W.-S.", Design of a plug-in type repetitive controller for periodic inputs," *IEEE Transactions on Control Systems Technology* **10**(4), 547–555 (2002).

[21] Srinivasan, K. and Shaw, F.-R.", Analysis and design of repetitive control systems using the regeneration spectrum," **113**(2), 216 (1991).